Chapter 2
Tools for Assessing the Damage Tolerance of Primary Structural Components

R. Jones and D. Peng

Abstract Fatigue considerations play a major role in the design of optimised flight vehicles, and the ability to accurately design against the possibility of fatigue failure is paramount. However, recent studies have shown that, in the Paris Region, cracking in high-strength aerospace quality steels and Mil Annealed Ti–6AL–4V titanium is essentially *R* ratio independent. As a result, the crack closure and Willenborg algorithm's available within commercial crack growth codes are inappropriate for predicting/assessing cracking under operational loading in these materials. To help overcome this shortcoming, this chapter presents an alternative engineering approach that can be used to predict the growth of small near-micron-size defects under representative operational load spectra and reveal how it is linked to a prior law developed by the Boeing Commercial Aircraft Company. A simple method for estimating the S–N response of 7050-T7451 aluminium is then presented.

Keywords Fatigue crack growth · Fatigue modelling · Life prediction · Similitude

2.1 Introduction

To achieve their design requirements, modern military make extensive use of aluminium, high-strength steels, that is, 4340 and D6ac, and titanium. The Joint Strike Fighter (F-35), the Super Hornet and the F/A-18 make extensive use of 7050-T7451 aluminium. However, there has been an increasing use of titanium in primary structural members due to its high strength, light weight, and good fatigue and fracture toughness properties. As a result, bulkheads in the F-22, the Super Hornet, the Swiss F/A-18, and the Joint Strike Fighter are made of titanium. In the F-22, titanium accounts for ∼36%, by weight, of all structural materials used in the aircraft.

R. Jones (✉)
Department of Mechanical and Aerospace Engineering, DSTO Centre of Expertise for Structural Mechanics, Monash University, Victoria 3800, VIC, Australia
e-mail: rhys.jones@eng.monash.edu.au

B. Farahmand (ed.), *Virtual Testing and Predictive Modeling*,
DOI 10.1007/978-0-387-95924-5_2, © Springer Science+Business Media, LLC 2009

Until recently, it had been thought that fatigue crack growth in 7050-T7451, high-strength aerospace steels and titanium was well understood. However, in his review of fatigue crack growth under variable amplitude loading, Skorupa [1] concluded that, viz:

> Experimental results also suggest that the underlying causes of load interaction phenomena are not necessarily similar for different groups of metals, e.g. steels of and Al and Ti alloys.

Furthermore, as a result of the Australian Defence Science and Technology Organisation's Flaw IdentificatioN through the Application of Loads (FINAL) testing program [2] it is now known [3, 4] that similitude-based concepts on which the crack growth programs AFGROW, NASGRO, and FASTRAN are based cannot be used to accurately predict the growth of near-micron-size flaws in 7050-T7451 aluminium alloy under representative in-flight loading. In this context it should also be noted that Forth, James, Johnston, and Newman [5] have reported that crack growth data obtained for D6ac and 4340 steels using compact tension (CT) specimens tested in accordance with the ASTM standards exhibited no R ratio dependency and hence no closure in the Paris region (Region II), see Fig. 2.1.

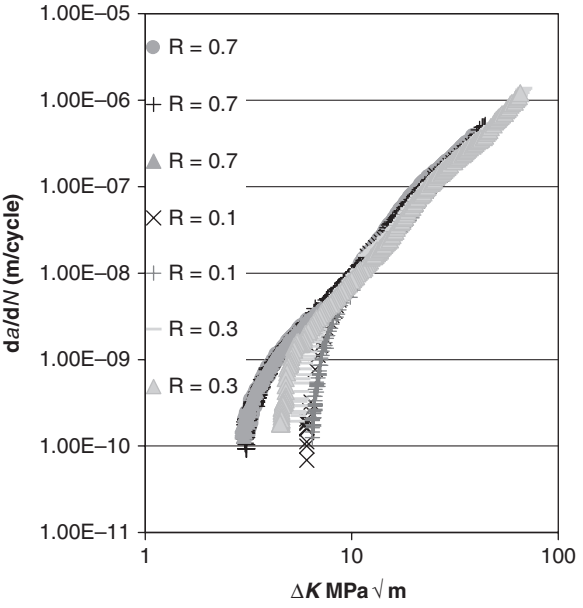

Fig. 2.1 Fatigue crack growth data from D6AC steel. Plot reproduced from [5]

This behaviour, that is, the da/dN versus ΔK relationship appearing to be R ratio dependent in Region I but showing no R ratio dependence and hence no closure in the Paris region, is also evident in the work of James and Knott [6] who studied cracking in QIN (HY80) steel, see Fig. 2.2.

As such, the various closure-based models and the Willenborg crack growth law, which models load interaction and sequence effects by modifying the effec-

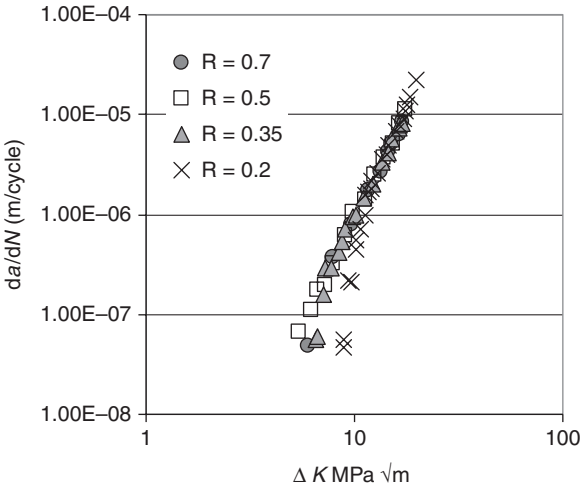

Fig. 2.2 Fatigue crack growth data from QIN (HY80) steel. Plot reproduced from [6]

tive *R* ratio, available within these codes cannot be used to accurately predict crack growth in high-strength steels. Jones, Farahmad, and Rodopoulos [7] have revealed that Mil Annealed Ti–6AL–4V titanium has a similar (near) *R* ratio independence. As such the various closure-based models and the Willenborg crack growth law cannot be used to accurately predict crack growth in Ti–6AL–4V. (This *R* ratio independence has also been seen in crack growth in rail steels [8] which have also been found to conform to the generalised Frost–Dugdale crack growth law [8, 9].)

When addressing the question of crack growth under representative in-service loading it should also be noted that in the review paper on crack growth and similitude Davidson [10] concluded that similitude was lost during fatigue crack growth under variable amplitude loading and stated that: "Detailed measurements of fatigue cracks undergoing simple load spectra confirm that when ΔK_{eff} is based on K_{open}, good correlations are achieved with large crack growth data.This understanding, although useful, does not easily translate to an engineering method for computing crack growth rate under complex variable amplitude loading."

The question thus arises: How can a valid virtual assessment of the performance of an aircraft/rail component under representative operational loading be performed if the fundamental concepts inherent in the existing crack growth codes, viz: AFGROW, FASTRAN, and NASGROW, do not apply to the materials from which the component fabricated, that is, for components made out of 4340 and D6ac steel, QIN (HY80) steel, rail steels, Mil Annealed Ti–6AL–4V, STOA Ti–6AL–4V, etc.? This chapter presents one possible approach which is based on the equivalent block formulation presented in [8, 11, 18] and reveals how it is linked to spectra where the constant amplitude Region II growth mechanism tends to be suppressed and a single value of C^* can be used to predict the crack length versus cycles history.

2.2 An Equivalent Block Method for Predicting Fatigue Crack Growth

It is now known that the mechanisms underpinning crack growth under variable amplitude load differ from those seen under constant amplitude loading [12]. It is also known that many materials either follow a non-similitude-based crack growth law [3, 4, 8, 9], lose similitude as the crack grows [10], or exhibit a near R ratio independence in the Paris Region [5–8]. In these cases, crack growth under representative operational loading cannot be predicted using the concepts inherent in the existing crack growth codes, viz: AFGROW, FASTRAN, and NASGROW, since they do not apply to the materials from which the component is fabricated, and since the data used in these calculations are obtained from constant amplitude tests that may not reflect the mechanisms driving growth under the spectrum of interest [12]. However, many practical engineering problems, that is, cracking in rail and aircraft structures, involve complex load spectra that can be approximated by a number of repeating load blocks. Schijve [13], Gallagher, and Stalnaker [14], Miedlar, Berens, Gunderson, and Gallagher [15], Barsom and Rolfe [16] and Miller, Luthra, and Goranson [17] revealed that these repeated blocks of loads can, in certain circumstances, be treated as equivalent to load cycles. We now show how this concept, that is, an equivalent block approach, can be used to describe crack growth in Mil Annealed Ti–6AL–4V and D6ac steel under complex variable amplitude loading.

To this end let us consider the case of block loading, where each block consists of a spectrum with n cycles that have peak stresses of σ_i, $i = 1 \ldots n$, with the associated cyclic ranges being $\Delta\sigma_i$, $i = 1 \ldots n$. Let us also assume that:

(i) The slope of the a versus block curve has a minimal number of discontinuities.
(ii) There are a large number of blocks before failure.

With these assumptions, Jones and Pitt [18] derived an "equivalent block" variant of the generalised Frost–Dugdale crack growth law [4, 8] to account for the crack growth per block, da/dB, viz

$$\mathrm{d}a/\mathrm{d}B = \tilde{C} {K_{\max}}^{\gamma} a^{1-\gamma/2} \tag{2.1}$$

where $\tilde{C}$ is a spectra-dependent constant and $K_{\max}$ is the maximum value of the stress intensity factor in the block. (The precise relationship between $\tilde{C}$ and the constant of proportionality in the Paris crack growth law is yet to be determined.) Jones, Molent, and Krishnapillai [11] subsequently extended this "equivalent block" law to have a form consistent with regions I, II, and III, viz

$$\mathrm{d}a/\mathrm{d}B = (\tilde{C} a^{1-\gamma/2} {K_{\max}}^{\gamma} - \mathrm{d}a/\mathrm{d}B_o)/(1.0 - K_{\max}/K_c) \tag{2.2}$$

where a is now the average crack length in the block, and K_{c} is the apparent cyclic fracture toughness. Here, as described in [11], the term da/dB_{o} reflects the both nature of the discontinuity from which the crack initiates and the apparent fatigue

threshold for this particular block loading spectra. However, it should (again) be stressed that this variant of the generalised Frost–Dugdale law is only applicable to crack growth data where the slope of the a versus block curve has minimal discontinuities and there are a large number of blocks to failure, see [8, 11, 18]. This formulation is (extensively) validated in [8, 11].

At this stage it is important to note that Miller, Luthra, and Goranson [17], at the Boeing Commercial Aircraft Company, have also developed a related (non-similitude) approach whereby instead of Equation (2.2) da/dB was expressed as

$$\mathrm{d}a/\mathrm{d}B = C(K/\mathrm{g}(a/\mathrm{t}))^m \tag{2.3}$$

where the function $g(a/t)$, which is a function of ratio of the crack length (a) to the thickness (t) of the specimen, was experimentally determined and its functional form is presented in [17]. This formulation was necessary to enable the predictions to match the measured crack length histories. However, Jones, Pitt, and Peng have shown [8] that the experimental test data used in [17] to determine the function $g(a/t)$ followed the generalised Frost-Dugdale crack growth law so that the two methodologies essentially coincide.

In the next section we present three examples that illustrate how the present non-similitude approach, that is, Equation (2.2), can be used to accurately predict crack growth in 7050-T7451, D6ac steel, and Mil Annealed Ti–6AL–4V aluminium specimens subjected to complex variable amplitude load spectra.

2.3 Fatigue Crack Growth under Variable Amplitude Loading

The first problem considered is that of crack growth in the 1969 General Dynamics, now Lockheed Martin Tactical Aircraft Systems (LMTAS), F-111 wing fatigue tested under a representative F-111 usage spectra. (An early F-111 in-flight failure was largely responsible for the USAF adopting a damage tolerance approach.) In this test, cracking was measured at a cut-out location designated as fuel flow hole 58 [19] on the lower (tension) surface of the D6ac steel wing pivot fitting, see Figs. 2.3 and 2.4.

Before attempting to predict crack growth in the pivot fitting we first confirmed that growth in D6ac steel conformed to the generalised Frost–Dugdale law. This was done via a collaborative project with Dr. Scott Forth at NASA [20]. As part of this project we examined the results of a detailed NASA study into crack growth in D6ac steel CT specimens. The test matrix evaluated is given in Table 2.1.

In this study it was found, see Fig. 2.5, that if we restrict ourselves to regions where $K_{\max} < 115.0$ Ksi $\sqrt{\text{in}}$ ($= 125$ MPa $\sqrt{\text{m}}$) then the data conforms to the generalised Frost–Dugdale crack growth law, viz

$$\mathrm{d}a/\mathrm{d}N = 8.12 \times 10^{-9}\, a^{(1-\gamma/2)}(\Delta\kappa)^{\gamma} - 2.79 \times 10^{-7} \tag{2.4}$$

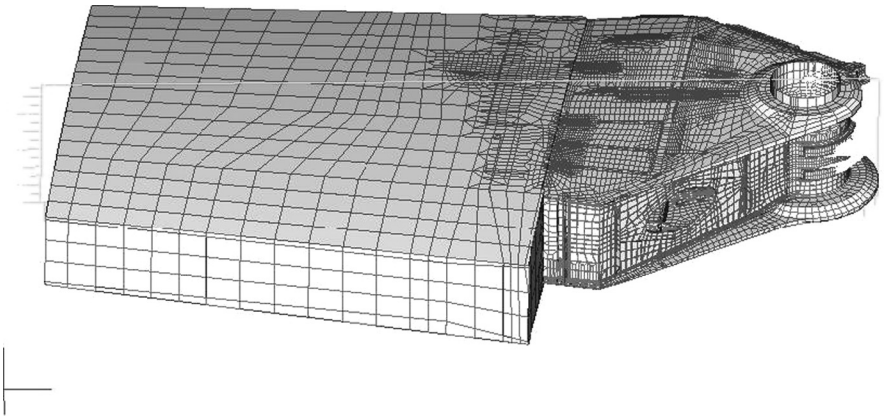

Fig. 2.3 Full 3D F-111 model, from DSTO

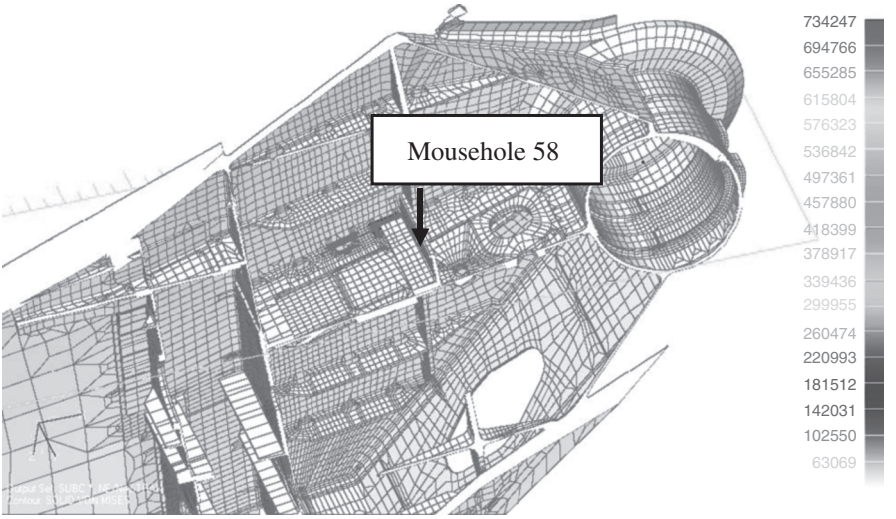

Fig. 2.4 Interior of the DSTO 3D F111 model

where the value of $\gamma = 2.6$ was taken from Murtagh and Walker [19] and where as per Walker [21] we have defined the crack driving force as

$$\Delta\kappa = {K_{\max}}^{(1-p)} \Delta K^p \tag{2.5}$$

where a value of $p = 0.95$ was found to best collapse the data. This low value of p confirmed the finding reported in [5] that the crack increment per cycle (da/dN) essentially has no R ratio dependency.

Having established that crack growth in D6ac steel conforms to the Generalised Frost–Dugdale law we assumed that in the 1969 wing tests there was, as reported in

Table 2.1 Test matrix

		Test frequency Hz
Ct3-5-tl	Constant $K_{max} = 15$	18
Ct3-10b-lt	Constant $R = 0.3$ LI	20
Ct3-12-lt	Constant $R = 0.9$ LI	20
Ct3-25-lt	Constant $R = 0.7$ LI	20
Ct3-27-lt	Constant $R = 0.9$ LI	22
Ct3-29-lt	Constant $R = 0.3$ LI	10
Ct3-46-lt	$R = 0.1$ LI	20
Ct3-47-lt	$R = 0.8$ LI	10

LI = Load increasing test, K_{max} = constant K_{max} test.

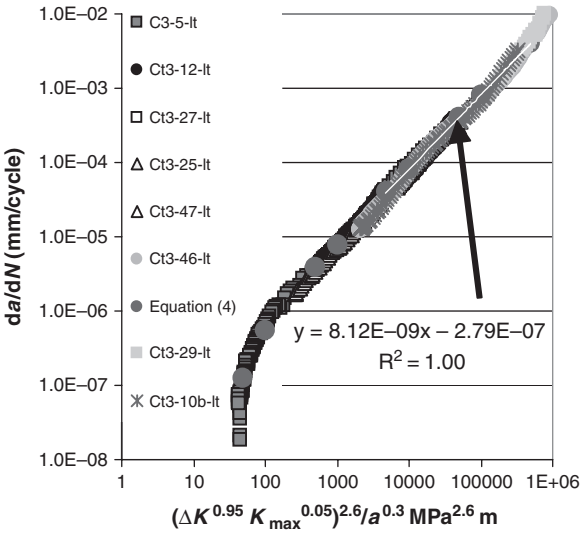

Fig. 2.5 Crack growth in D6ac steel, from [20]

[19], an initial 0.19-mm semi-circular flaw. At each increment of crack growth, the stress intensity factors were computed using a weight function technique together with the stress field determined from the finite element model shown in Figs. 2.3 and 2.4. Crack growth was then predicted using Equation (2.2) with $\gamma = 2.6$ and $K_C = 87$ MPa $\sqrt{}$m, as given in [19], and $\tilde{C} = 3.0 \times 10^{-6}$. The load spectra used in the 1969 test, and in this study, was provided by the Australian Defence Science and Technology Organisation (DSTO) and corresponds to that used in [19].

The resultant predicted crack depth histories are presented in Fig. 2.6 where we see good agreement between the predicted and the measured crack depth histories. In this example, when using Equation (2.2) to compute crack growth at the deepest point of the semi-elliptical surface flaw the quantity 'a' on the left- and the right-hand sides of Equation (2.2) is the crack depth. Similarly, when using Equation (2.2) to compute crack growth at the surface points, the quantity 'a' on the left- and the

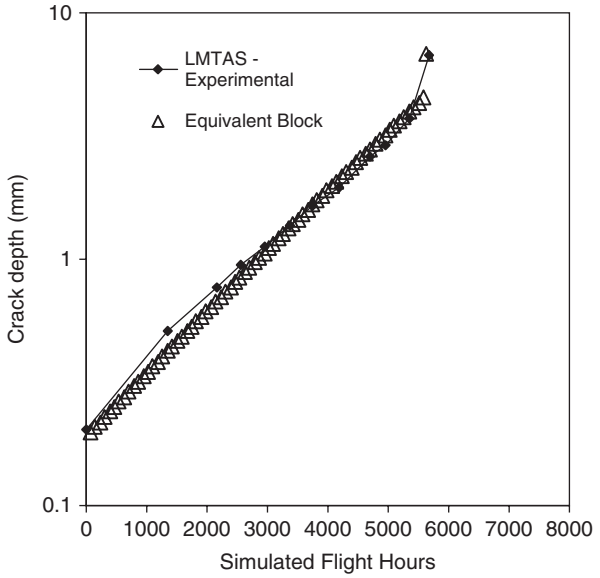

Fig. 2.6 Measured and predicted crack growth in the 1969 F-111 wing test

right-hand side of Equation (2.2) is the half crack surface length. In this fashion, we allow for the variation of the crack aspect ratio during crack growth.

2.3.1 Fatigue Crack Growth in an F/A-18 Aircraft Bulkhead

The next problem considered involved cracking in an F/A-18 Y488 bulkhead tested as part of the DSTO Flaw IdeNtification through the Application of Loads (FINAL) test program, see Dixon et al. [2]. This test program utilised ex-service Canadian Forces (CFs) and US Navy (USN) wing attachment centre barrel (CB) sections loaded using an industry-standard-modified mini-FALSTAFF spectrum, see [2], which is representative of flight loads seen by fighter aircraft. Since cracking in the bulkhead was three-dimensional, a three-dimensional FE model was required, see Figs. 2.7 and 2.8. The location of the crack is shown in Fig. 2.8, where node 4390 represents the centre of the initial semi-elliptical surface flaw. This problem had previously been studied using a cycle-by-cycle approach [4] and it was known that cracking in 7050-T7451 conformed to the generalised Frost–Dugdale law, [4, 22]. As in [4] we again used a weight function technique together with the stress field as determined from the FE model of the bulkhead to compute the associated stress intensity factors. The crack growth history from initial equivalent pre-crack sizes (EPS) of 0.003 mm was predicted using Equation (2.2) with $\gamma = 3.36$ and K_c of 35.4 MPa$\sqrt{\text{m}}$ as given in [4] and $\tilde{C} = 2.25 \times 10^{-10}$.

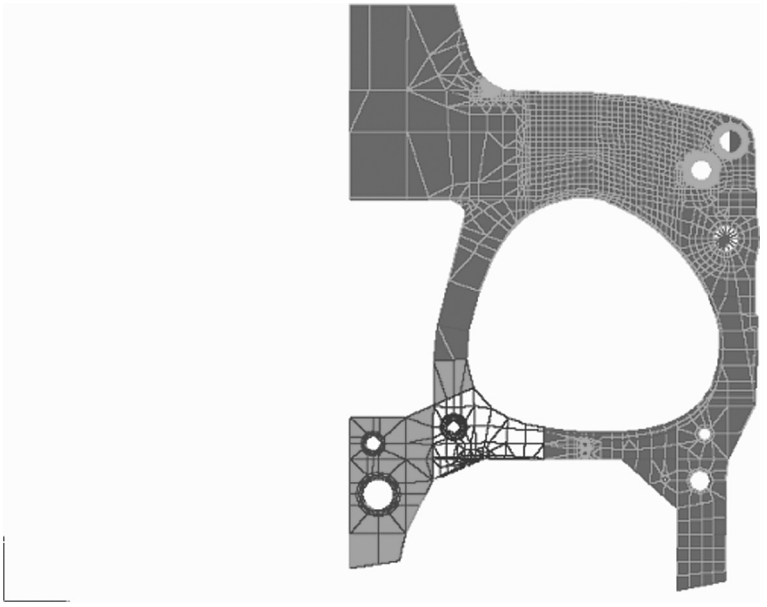

Fig. 2. 7 The bulkhead structure

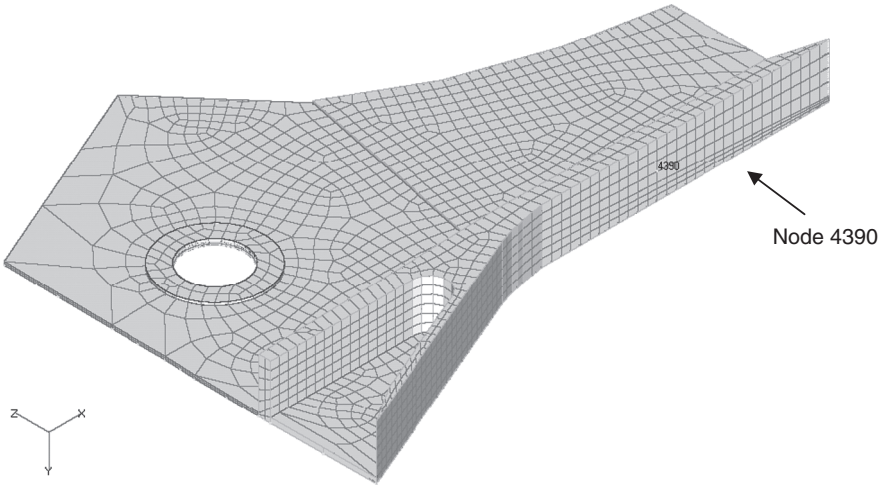

Fig. 2.8 The local mesh

The predicted crack depth history, allowing for changes in the aspect ratio of the flaw as the crack grows, is shown in Fig. 2.9 together with the associated experimental test result, where we see that there is very good agreement. Figure 2.9 also contains a comparison with predictions, presented in [4], made using FASTRAN II. Here we see that FASTRAN II predicted a very long fatigue life. Furthermore,

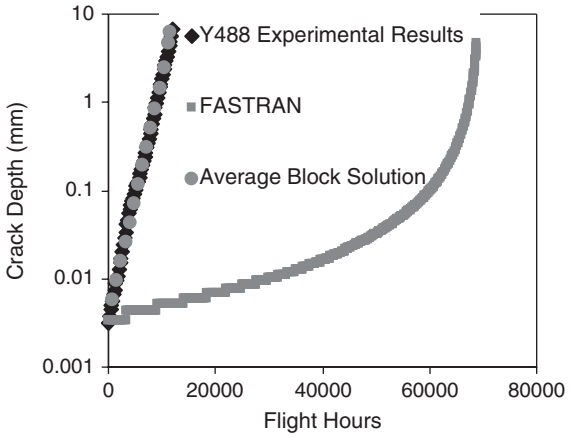

Fig. 2.9 Experimental and predicted crack growth histories

the shape of the crack depth versus cycles curve predicted by FASTRAN II differed markedly from the test data. In Fig. 2.9 we see that the experimental and predicted (from Equation 2.2) crack depth histories show a behaviour that is consistent across three decades of crack lengths, that is, from 0.003 mm to more than 5 mm.

2.3.2 Crack Growth in Mil Annealed Ti–6AL–4V under a Fighter Spectrum

Jones, Farahmad, and Rodopoulos [7], who analysed the data presented in [23, 24], found that crack growth in Mil Annealed Ti–6AL–4V titanium was essentially R ratio independent, see Fig. 2.10. Figure 2.10 shows that cracking in Mil Annealed Ti-6AL-4V also appears to conform to the generalised Frost–Dugdale law, viz

$$\mathrm{d}a/\mathrm{d}N = C^* a^{(1-\gamma/2)}\,(\Delta\kappa)^{\gamma} - \mathrm{d}a/\mathrm{d}N_0 \tag{2.6}$$

with $\Delta\kappa$ as given in Equation (2.5) $C^* \sim 2.5\ 10^{-11}$, $\gamma = 2.5$, $p = 0.08$, $K_c = 100$ MPa $\sqrt{\mathrm{m}}$ and $\mathrm{d}a/\mathrm{d}N_0 = 4.45 \times 10^{-9}$. As explained in [4, 8, 9] the term $\mathrm{d}a/\mathrm{d}N_0$ reflects both the nature of the discontinuity from which the crack initiates and the apparent fatigue threshold. The small value of p reveals that crack growth in Mil Annealed Ti–6AL–4V titanium has a very weak R ratio dependency. We also see that this relationship, that is, Equation (2.6), holds over 3 orders of magnitude, that is, $2 \times 10^{-9} < \mathrm{d}a/\mathrm{d}N < 2 \times 10^{-6}$. It should also be noted that this value of γ compares well with that of $\gamma = 2.6$ obtained by Zhuang et al. [25] for Mil Annealed Ti–6AL–4V tested under spectrum loading.

With this in mind let us now examine the crack growth data presented by Northrop-Grumman [26] who studied crack growth in 6-inch-wide and 0.289-inch-thick centre cracked Mil Annealed Ti-6AL–4V panels subjected to a fighter load

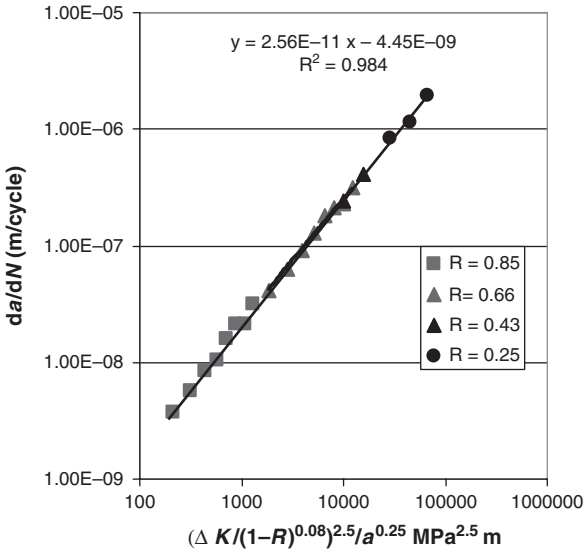

Fig. 2.10 Crack growth in Mil-Annealed Ti–6AL–4V, from [7]

spectrum with a peak remote stress of 103 ksi (710 MPa). The resultant predictions are shown in Fig. 2.11 where we again see an excellent agreement between the measured and the computed crack length histories. In this case, the left hand side of Equation (2.2) is da/d$Block$, $\tilde{C} = 2.83 \times 10^{-10}$, $\gamma = 2.5$, and $K_c = 150$ ksi $\sqrt{\text{in}}$ (163 MPa $\sqrt{\text{m}}$).

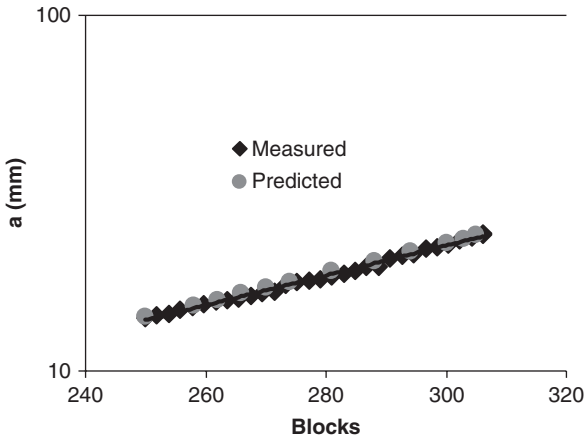

Fig. 2.11 Grumman centre cracked panel crack growth under a fighter spectra

The above examples illustrate how the equivalent block method may be used to simulate crack growth under variable amplitude loading both for aluminium alloys and for the materials that exhibit minimal R ratio dependency. However, it must be stressed that this approach has a number of fundamental requirements, viz:

(i) There are a large number of blocks before failure.
(ii) The slope of the a versus block curve has a minimal number of discontinuities.

Applications of this methodology to a range of aluminium alloys as well as to cracking under a Helicopter load spectra and spectra corresponding to several control points in the Joint Strike Fighter are given in [8, 11, 27, 28].

White, Barter, and Molent [12] studied block loading which consisted of a large number of variable amplitude loads interspersed with a single block of constant amplitude loading. They found that at the onset of the constant amplitude loading, the crack changed planes and subsequently reverted back to its original plane after the constant amplitude loading ceased. This indicated that the mechanism's driving constant amplitude and variable amplitude loading differed and that, in the Paris region, the constant amplitude mechanism was suppressed during variable amplitude loading. This observation explains why, in the examples presented above, only one value of C^* is needed to represent crack growth. At this stage it should be noted that Liu [29] has shown that the Frost–Dugdale law has different slopes in regions I and II. Tiong and Jones [30] revealed that for aluminium alloys the value of C^* in Region II is approximately 5 times its Region I value. However, when the Region II growth mechanism is suppressed crack growth can be predicted using the C^* value associated with Region I.

2.4 A Virtual Engineering Approach for Predicting the S–N Curves for 7050-T7451

Section 2.1 when taken together with the cycle-by-cycle study presented by Jones, Molent, and Pitt [4] illustrates the ability of the Generalised Frost–Dugdale law to simulate the growth of near-micron-size flaws in 7050-T7451 aluminium alloy. As a result, it is possible to use this formulation to derive the S–N curve for 7050-T7451. To illustrate this approach let us assume that the material contains a small semi-circular surface initial defect and that it retains this semi-circular shape during growth. Then

$$\Delta K = F\Delta\sigma\sqrt{(a\pi)} \tag{2.7}$$

where $\Delta\sigma$ is the remote stress, F is a geometry factor, also termed β, which is also commonly called a boundary correction factor. For a small three-dimensional semi-elliptical surface flaw we can approximate F as

$$F = 2 \times 1.12/\pi \tag{2.8}$$

so that

$$\Delta K = (2 \times 1.12/\pi)\Delta\sigma\sqrt{(a/\pi)} \tag{2.9}$$

To account for R ratio effects in aluminium alloys under constant amplitude loading, we will adopt Newman's [31] proposal that ΔK be replaced by ΔK_{eff}, which for the present problem we can express as

$$\Delta K_{\text{eff}} = (1 - \sigma_o/\sigma_{\max})(2 \times 1.12\, \sigma_{\max}\sqrt{(a/\pi)}) \tag{2.10}$$

where σ_{o} is the so-called "crack opening stress", see Appendix. However, when performing crack growth calculations for surface flaws, FASTRAN-II [31] only uses 0.9 of this value, that is,

$$\Delta K_{\text{eff}}(\text{in calcs.}) = 0.9(1 - \sigma_o/\sigma_{\max})(2 \times 1.12\, \sigma_{\max}\, \sqrt{(a/\pi)}) \tag{2.11}$$

so that

$$\mathrm{d}a/\mathrm{d}N = C^*(0.9(1 - \sigma_o/\sigma_{\max})(2 \times 1.1.2\, \sigma_{\max}/\sqrt{\pi})))^{\gamma} a \tag{2.12}$$

Integrating Equation (2.12) gives

$$N = \ln(a_{\text{f}}/a_{\text{i}})/C^*(2 \times 0.91.12 \times (1 - \sigma_o/\sigma_{\max})\sigma_{\max}/\sqrt{(\pi)})^{\gamma} \tag{2.13}$$

where a_{i} is the initial defect size, which as shown by Molent et al. [32], for 7050-T7451 aluminium has a mean value of ~10 microns and a_{f} is the crack size at failure.

2.4.1 Computing the Endurance Limit

If we say that there will be no growth if the computed value of da/dN (at the initial flaw size a_{i}) is less than a critical value then this will give an endurance stress. In this work we will take this value to be between 1–2 $\times$ 10^{-10} m/cycle. This produces a different endurance limit for each stress.

For 7050-T7451 $C^* = 1.21 \times 10^{-12}$ and $\gamma = 3.36$. The resultant predicted S–N curve is plotted in Fig. 2.12 along with the associated Mil Handbook 5 S–N curve. Note that the yield stress for this material in the thick plate condition is in the range 455–496 MPa (66–72 ksi).

2.5 Conclusion

The Australian Defence Science and Technology Organisation's Flaw IdentificatioN through the Application of Loads (FINAL) testing program revealed that the crack growth programs AFGROW, NASGRO, and FASTRAN cannot be used to accurately predict the growth of near-micron-size flaws in 7050-T7451 aluminium alloy under representative in-flight loading. This paper has shown that the Region II crack growth data reveals that cracking in high-strength aerospace quality steels and

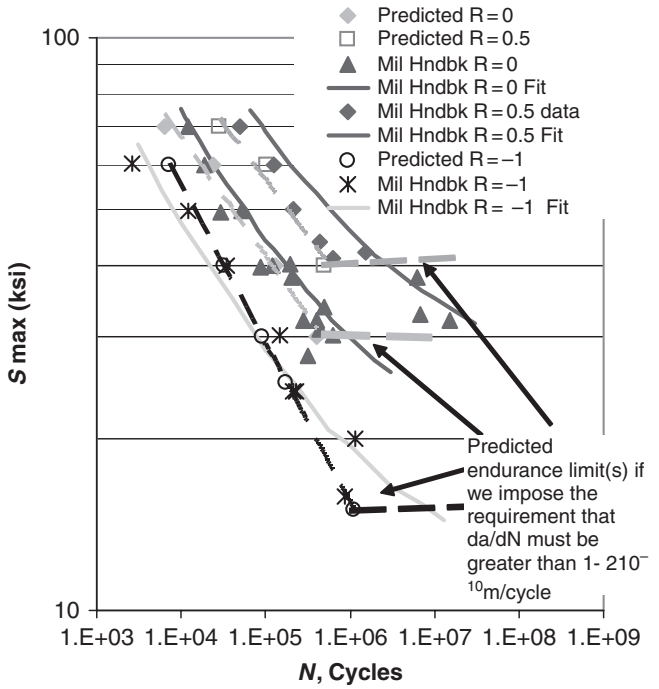

Fig. 2.12 Measured and predicted S–N curves for 7050-T7451 aluminium alloy

Mil Annealed Ti–6AL–4V titanium is essentially *R* ratio independent. As a result, the crack closure and Willenborg algorithm's available within commercial crack growth codes are also inappropriate for predicting/assessing cracking under operational loading in these materials. To help overcome this shortcoming this chapter has presented an alternative engineering approach that is linked to the formulation developed by the Boeing Commercial Aircraft Company, which can be used to predict the growth of small near-micron-size defects under representative operational load spectra. This approach:

i. is generally consistent with experimental results,
ii. can be used to predict crack growth from near-micron-size initial flaws, and
iii. has the potential to accurately predict crack growth in real aircraft structures under complex load spectra.

However, it should be stressed that this variant of the Generalised Frost–Dugdale law is only applicable to crack growth data where the slope of *a* versus block curve has minimal discontinuities and there are a large number of blocks to failure. In such cases the constant amplitude Region II growth mechanism tends to be

suppressed and a single value of C^* can be used to predict the crack length versus cycles history.

Acknowledgments This work was performed under the auspices of the DSTO Centre of Expertise in Structural Mechanics which is supported by the RAAF Directorate General Technical Airworthiness Air Structural Integrity Section. We specifically acknowledge the support given by Lorrie Molent, Functional Head Combat Aircraft (Structural Integrity), Dr Weiping Hu, Science Team Leader: Structural Lifing Methods and Tools, Dr. Scott Forth at the NASA Johnson Space Center, Prof. Chris Rodopoulos at the University of Patras, Greece, and the Materials and Engineering Research Centre, Sheffield Hallam University, England, and Dr. Bob Farahmand at TASS (Los Angeles).

Appendix: Formulae for Computing the Crack Opening Stress

Newman [31] defined an opening load, which he denoted as S_0, as:

$$S_0/S_{max} = \mathrm{A}_0 + \mathrm{A}_1 R + \mathrm{A}_2 R^2 + \mathrm{A}_3 R^3 \text{ for } R \geq 0 \tag{2.14}$$

and

$$S_0/S_{max} = \mathrm{A}_0 + \mathrm{A}_1 = R \text{ for } R < 0 \tag{2.15}$$

for $S_{\max} < 0.8\sigma_0$, $S_{\min} > -\sigma_0$, where $S_{\max}$ and $S_{\min}$ are the maximum minimum stress in the cycle and σ_0 is the yield stress. If $S_0/S_{\max}$ is less than R then $S_0 = S_{\min}$, whilst if $S_0/S_{\max}$ is negative then $S_0/S_{\max} = 0.0$.

The A_j coefficients in Equations (2.14) and (2.15) are functions of α, the constraint factor, and $S_{\max}/\sigma_0$ and are given in [31] as:

$$\mathrm{A_o} = (0.825 - 0.34\alpha + 0.05\alpha^2)[\mathrm{COS}(\pi \mathrm{S_{max}F}/2\sigma_0]^{1/\alpha}$$

$$\mathrm{A_1} = (0.415 - 0.071\alpha)\mathrm{S_{max}F}/\sigma_0$$

$$\mathrm{A_2} = 1 - \mathrm{A_0} - \mathrm{A_1} - A3$$

$$\mathrm{A_3} = 2\mathrm{A_0} + A_1 - 1 \tag{2.16}$$

for $\alpha = 1$ to 3.

The boundary correction factor, F, accounts for the influence of finite width on the stresses required to propagate the crack. For 3D small 3D surface cracks we can approximate F as $F \sim 2 \times 1.12/\pi$.

References

1. M. Skorupa, “Load Interaction Effects During Fatigue Crack Growth Under Variable Amplitude Loading—A Literature Review. Part II: Qualitative Interpretation,” Fatigue Fract. Eng. Mater. Struct., Vol. 22, 1999, pp. 905–926.
2. B. Dixon, L. Molent, and S.A. Barter, “The FINAL program of enhanced teardown for agile aircraft structures,” Proceedings of 8th NASA/FAA/DOD Conference on Aging Aircraft, Palm Springs, 31 Jan–3 Feb, 2005.
3. L. Molent, R. Singh, and J. Woolsey, “A method for evaluation of in-service fatigue cracks,” Eng. Fail. Anal., Vol. 12, 2005, pp. 13–24.
4. R. Jones, L. Molent, and S. Pitt, “Crack growth from small flaws,” Int. J. Fatigue, Vol. 29, 2007, pp. 658–1667.
5. S.C. Forth, M.A. James, W.M. Johnston, and J.C. Newman, Jr., “Anomolous Fatigue Crack Growth Phenomena in High-strength Steel,” Proceedings Int. Congress on Fracture, Italy, 2007.
6. M.N. James and J.F. Knott, “An Assessment of Crack Closure and the Extent of the Short Crack Regime in QlN (HY80) Steel,” Fatigue Frac. Eng. Mater. Struc., Vol. 8, No. 2, 1985, pp. 177–191.
7. R. Jones, B. Farahmand, and C. Rodopoulos, “Fatigue crack growth discrepencies with stress ratio,” Theor. Appl. Frac. Mech., doi: 10.1016/tafmec.2009.01.004.
8. R. Jones, S. Pitt, and D. Peng, “The Generalised Frost–Dugdale Approach to Modeling Fatigue Crack Growth,” Eng Fail Anal, 15, 2008, pp. 1130–1149.
9. R. Jones, B. Chen, and S. Pitt, “Similitude: Cracking in Steels,” Theor. Appl. Frac. Mech., Vol. 48, No. 2, pp. 161–168.
10. D.L. Davidson, “How Fatigue Cracks Grow, Interact with Microstructure, and Lose Similitude,” Fatigue and Fracture Mechanics: 27th Volume, ASTM STP 1296, R.S. Piascik, J.C. Newman, and N.E. Dowling, Eds., American Society for Testing and Materials, 1997, pp. 287–300.
11. R. Jones, L. Molent, and K. Krishnapillai, “An Equivalent Block Method for Computing Fatigue Crack Growth,” Int. J. Fatigue, Vol. 30, 2008, pp. 1529–1542.
12. P. White, S.A. Barter, and L. Molent, “Observations of Crack Path Changes Under Simple Variable Amplitude Loading in AA7050-T7451,” Int. J. Fatigue, Vol. 30, 2008, pp. 1267–1278.
13. J. Schijve, “Fatigue Crack Growth Under Variable-Amplitude Loading,” Eng. Frac. Mech., Vol. 11, 1979, pp. 207–221.
14. J.P. Gallagher and H.D. Stalnaker, “Developing Normalised Crack Growth Curves for Tracking Damage in Aircraft, American Institute of Aeronautics and Astronautics,” J. Aircraft, Vol. 15, No. 2, pp. 114–120.
15. P.C. Miedlar, A.P. Berens, A. Gunderson, and J.P. Gallagher, “Analysis and Support Initiative for Structural Technology (ASIST),” AFRL-VA-WP-TR-2003-3002, 2003.
16. J.M. Barsom and S.T. Rolfe, “Fracture and Fatigue Control in Structures: Applications of Fracture Mechanics,” Butterworth-Heinemann Press, 1999.
17. M. Miller, V.K. Luthra, and U.G. Goranson, “Fatigue Crack Growth Characterization of Jet Transport Structures,” Proc. of 14th Symposium of the International Conference on Aeronautical Fatigue (ICAF), Ottawa, Canada, 1987.
18. R. Jones, and S. Pitt, “Crack Patching: Revisited,” Comp. Struct., Vol. 32, 2006, pp. 218–223.
19. B.J. Murtagh and K.F. Walker, “Comparison of Analytical Crack Growth Modelling and the A-4 Wing Test Experimental Results for a Fatigue Crack in an F-111 Wing Pivot Fitting Fuel Flow Hole Number 58”, DSTO-TN-0108, 1997.
20. R. Jones and S.C. Forth, “Cracking In D6ac Steel,” Submitted J. Theor. Appl. Fract. Mech., 2008 (in press).

21. E.K. Walker, “The Effect of Stress Ratio During Crack Propagation and Fatigue for 2024-T3 and 7076-T6 Aluminium.” In: Effect of Environment and Complex Load History on Fatigue Life, ASTM STP 462, American Society for Testing and Materials, Philadelphia, 1970, pp. 1–14.
22. R. Jones, C. Wallbrink, S. Pitt, and L. Molent, “A Multi-Scale Approach to Crack Growth,” Proceedings Mesomechanics 2006: Multiscale Behavior of Materials and Structures: Analytical, Numerical and Experimental Simulation, Porto, Portugal, 2006.
23. C.M. Hudson, “Fatigue-Crack Propagation in Several Titanium and One Superalloy Stainless-Steel Alloys, NASA TN D-2331, 1964.
24. T.R. Porter, “Method of Analysis and Prediction for Variable Amplitude Fatigue Crack Growth,” Eng. Fract. Mech., Vol. 4, 1972, pp. 717–736.
25. W. Zhuang, S. Barter, L. Molent, “Flight-By-Flight Fatigue Crack Growth Life Assessment,” Int J Fatigue, Vol. 29, 2007, pp. 1647–165.
26. P.D. Bell and M. Creager, “Crack Growth Analysis For Arbitrary Spectrum Loading,” Volume I – Results and Discussion, Final Report: June 1972 – October 1974, Technical Report AFFDL-TR-74-129, 1974.
27. R. Jones, S. Pitt, and D. Peng, “An Equivalent Block Approach to Crack Growth,” In: Multiscale Fatigue Crack Initiation and Propagation of Engineering Materials: Structural Integrity and Microstructural Worthiness, G.C. Sih, Ed., ISBN 978-1-4020-8519, Springer Press, 2008.
28. L. Molent, S. Barter, and R. Jones, “Some Practical Implications of Exponential Crack Growth,” In: Multiscale Fatigue Crack Initiation and Propagation of Engineering Materials: Structural Integrity and Microstructural Worthiness, G.C. Sih, Ed., ISBN 978-1-4020-8519, Springer Press, 2008.
29. H.W. Liu, Crack Propagation in Thin Metal Sheet Under Repeated Loading, Wright Air Development Center, WADC TN, 1959, pp. 59–383.
30. U.H. Tiong and R. Jones, “Damage Tolerance Analysis of a Helicopter Component,” Int. J. Fatigue, 2008 doi:10.1016/j.ijfatigue.2008.05.012
31. J.C. Newman, Jr., FASTRAN-II- A fatigue Crack Growth Structural Analysis Program, NASA Technical Memorandum 104159, 1992.
32. L. Molent, Q. Sun and A.J. Green, “Characterisation of equivalent initial flaw sizes in 7050 aluminium alloy,” Fatigue Fract. Engng. Mater Struct., Vol. 29, 2006, pp. 916–937.

http://www.springer.com/978-0-387-95923-8

Virtual Testing and Predictive Modeling
For Fatigue and Fracture Mechanics Allowables
Farahmand, B. (Ed.)
2009, XXIII, 407 p., Hardcover
ISBN: 978-0-387-95923-8